Supporting Information

BODIPY-Conjugated Bis-terpyridine Ru(II) Complexes Showing Ultra-long Luminescent Lifetimes and Applying to Triplet-triplet Annihilation Upconversion

Xingke Yu,[†, a] Fanrui Gao,[†, a] Weiyi Zhao,[b] Hongxia Lai,[a] Lingling Wei,[a] Cheng Yang*[a] and Wanhua Wu*[a]

[a.] *Key Laboratory of Green Chemistry & Technology of Ministry of Education, College of Chemistry, Sichuan University, Chengdu 610064, China*

[b.] *Sichuan University-Pittsburgh Institute, Sichuan University, Chengdu 610064, China*

† X. Yu and F. Gao contributed equally to this work.

Table of Contents

1.0 Synthesis and characterizations

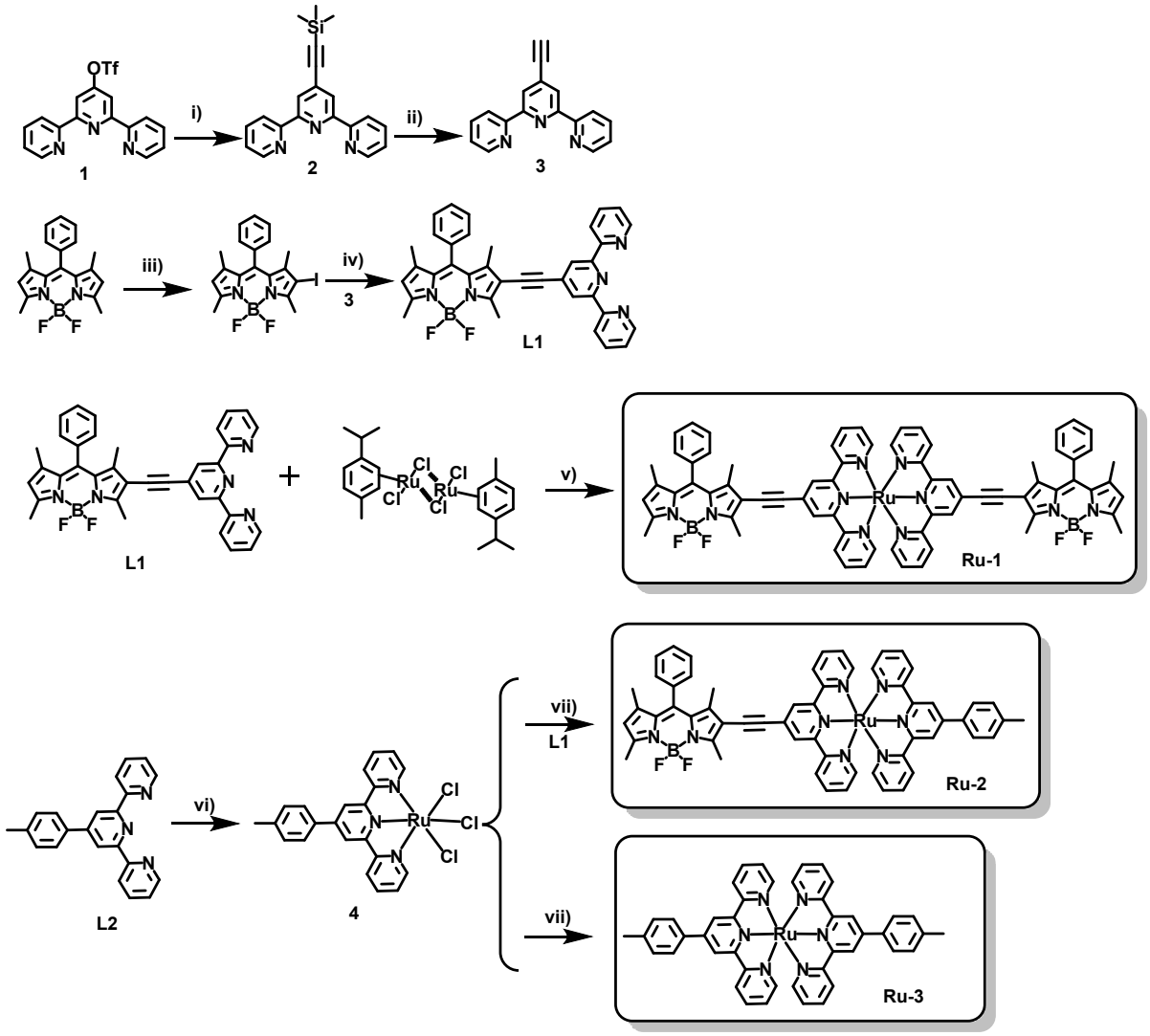

Scheme S1. The synthetic route of **Ru-1**, **Ru-2** and **Ru-3**. Reagents and conditions: (i) Pd $(PPh_3)_2Cl_2$, PPh_3, CuI, triethylamine/THF, 70℃, 4 h; (ii) KF, MeOH/THF, RT, overnight; (iii) NIS, CH_2Cl_2, RT, 30min; (iv) Pd $(PPh_3)_2Cl_2$, PPh_3, CuI, Triethylamine/THF, 70℃, overnight, N_2; (v) ethanol, 90℃, 48h, N_2; (vi) $RuCl_3$; ethanol, 90℃, 2h, N_2; (vii) 4-Ethylmorpholine, ethanol, 90℃, 48h, N_2.

2.0 NMR and MS spectra

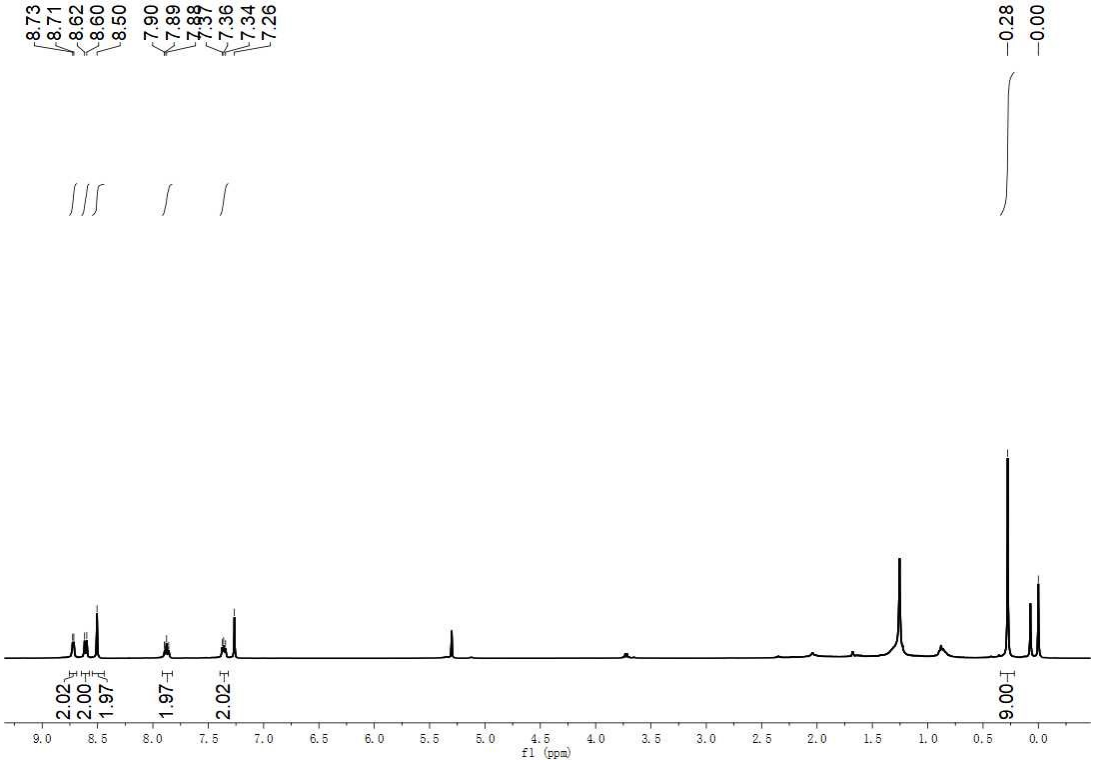

Figure S2. ^{1}H NMR for **2** in $CDCl_3$, 20°C.

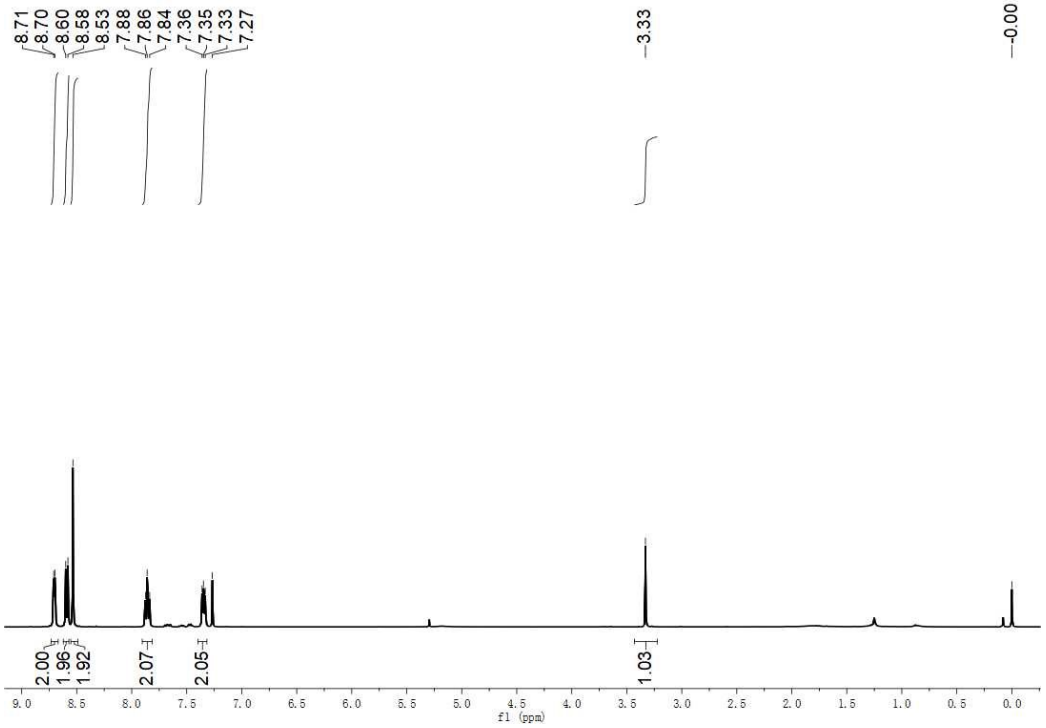

Figure S3. ^{1}H NMR for **3** in $CDCl_3$, 20°C.

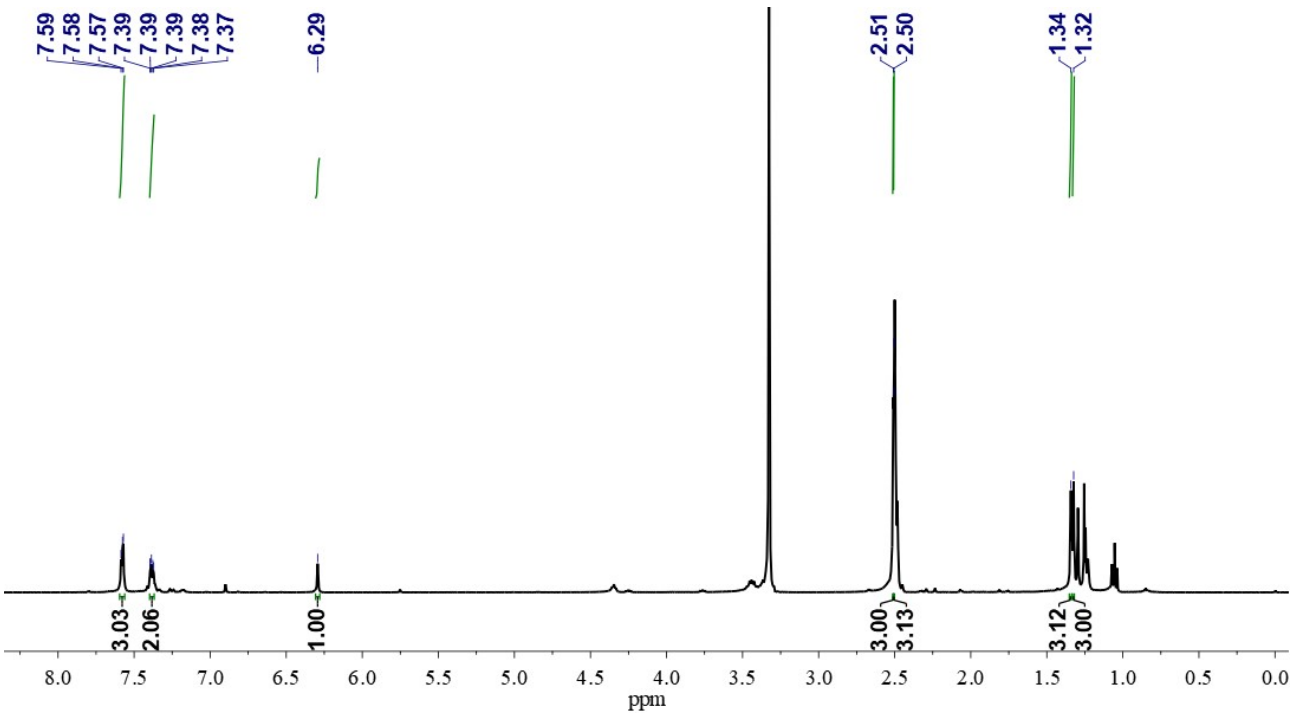

Figure S4. ^{1}H NMR for **Iodo-Bodipy** in CD_3OD, 20°C.

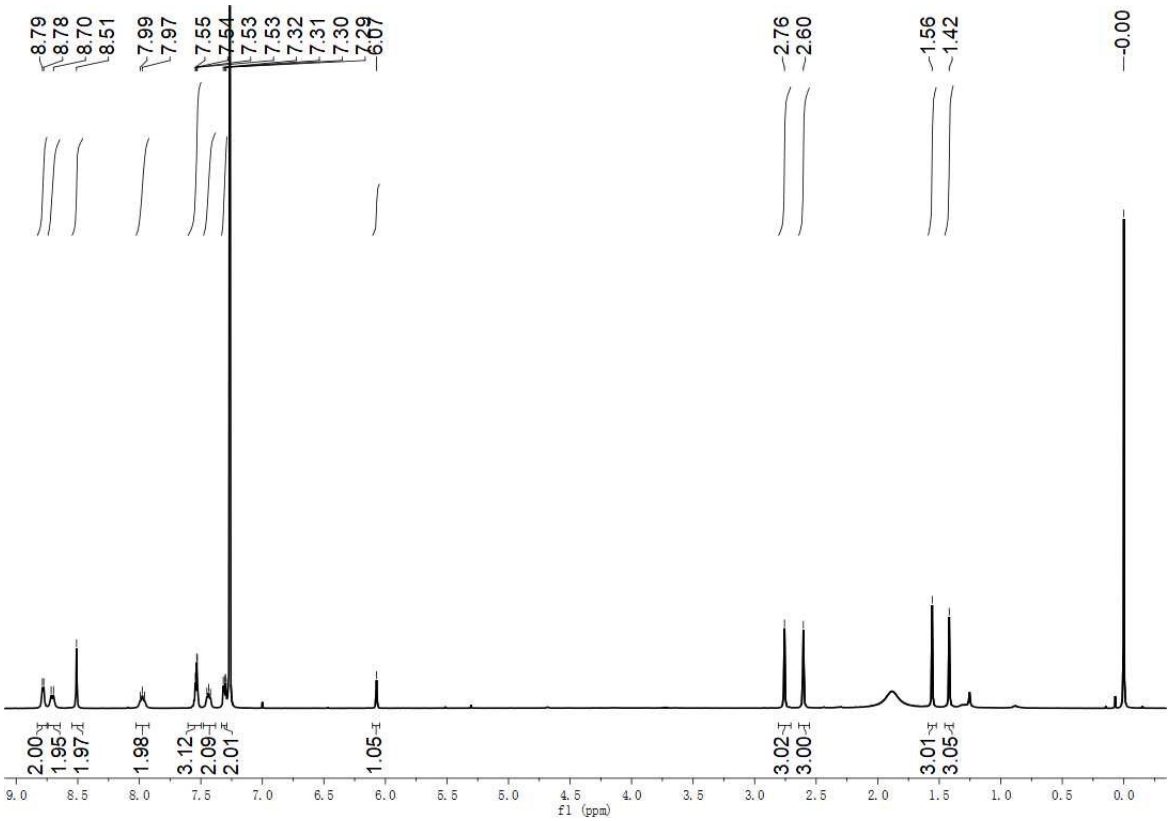

Figure S5. ^{1}H NMR for **L1** in $CDCl_3$, 20°C.

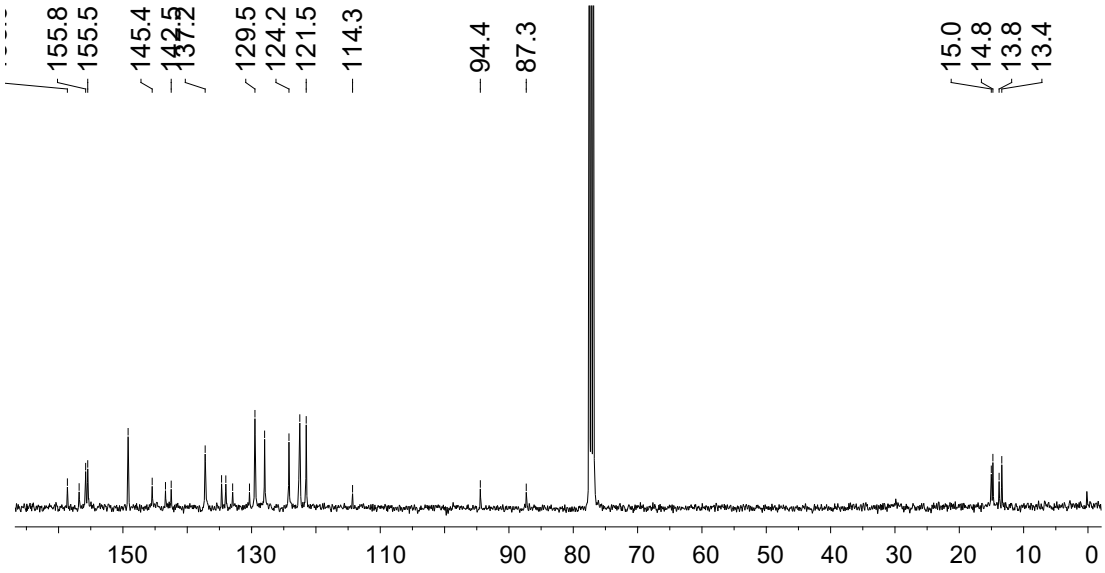

Figure S6. ^{13}C NMR for **L1** in $CDCl_3$, 20°C.

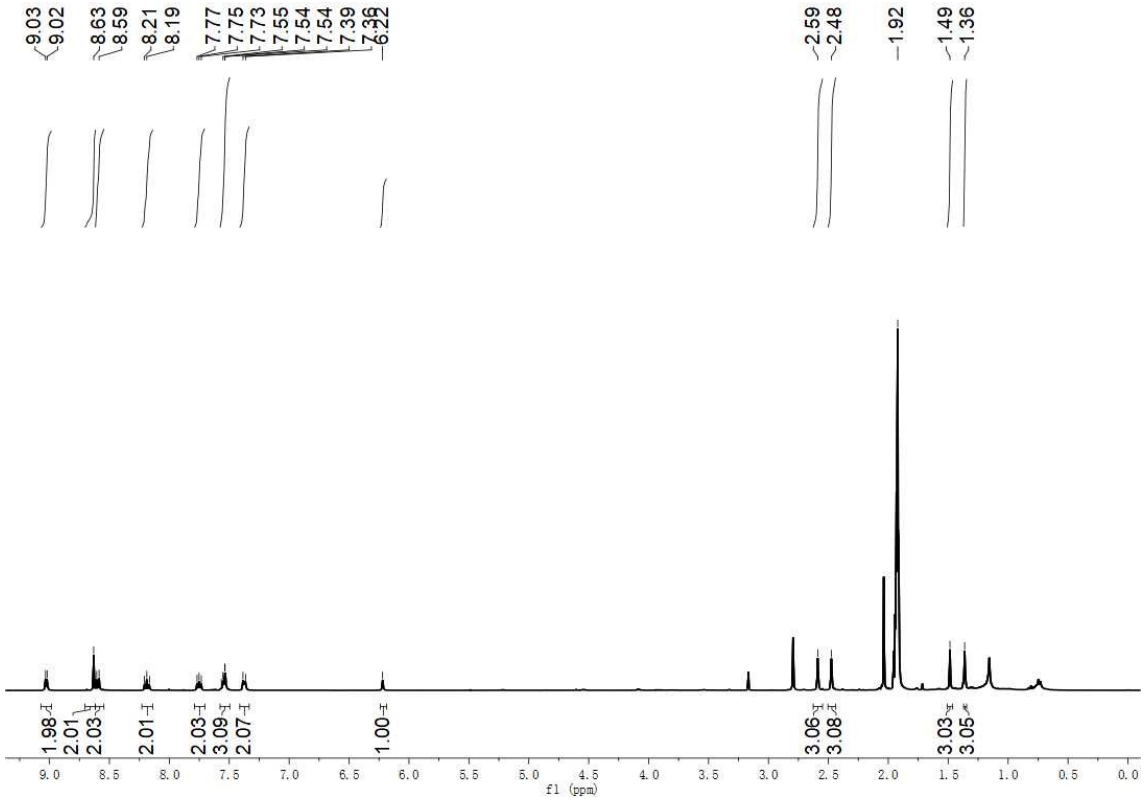

Figure S7. ^{1}H NMR for **Ru-1** in acetone-*d6*, 20°C.

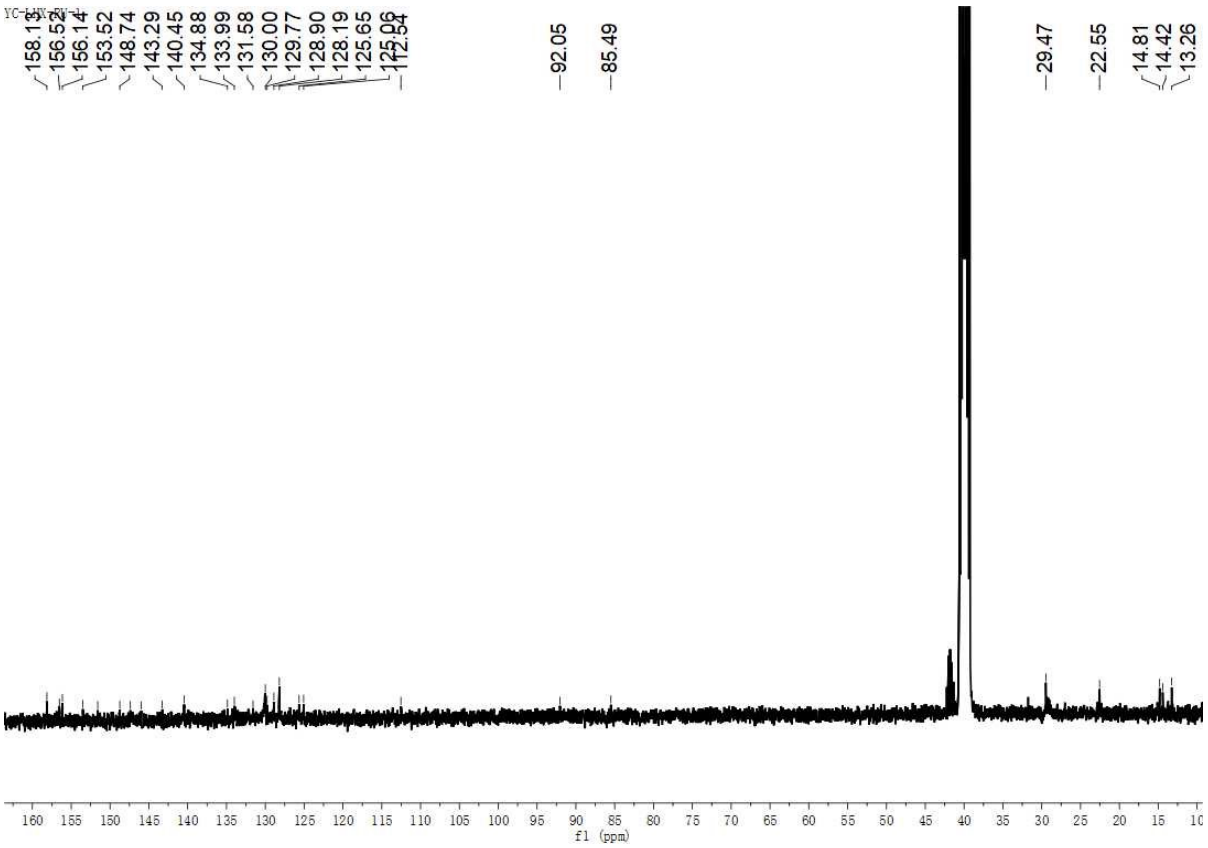

Figure S8. ^{13}C NMR for **Ru-1** in DMSO-*d6*, 20℃.

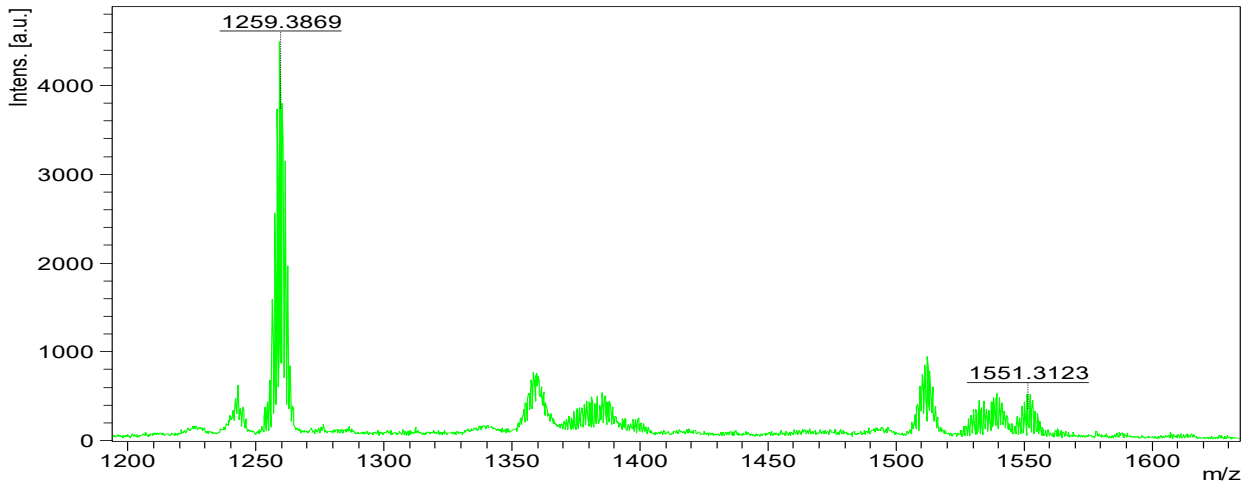

Figure S9. The MALDI-TOF (HRMS) spectrum of **Ru-1**.

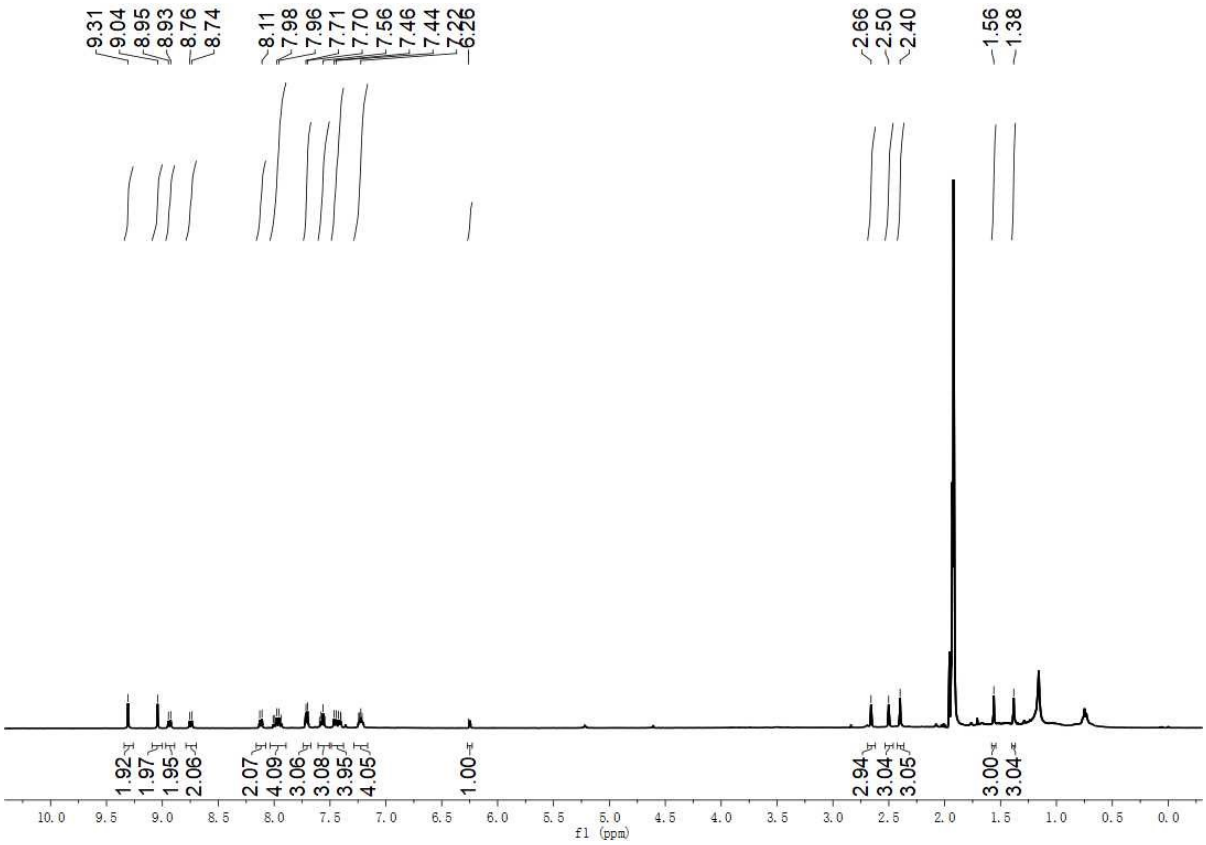

Figure S10**.** [1]H NMR for **Ru-2** in acetone-*d6*, 20℃.

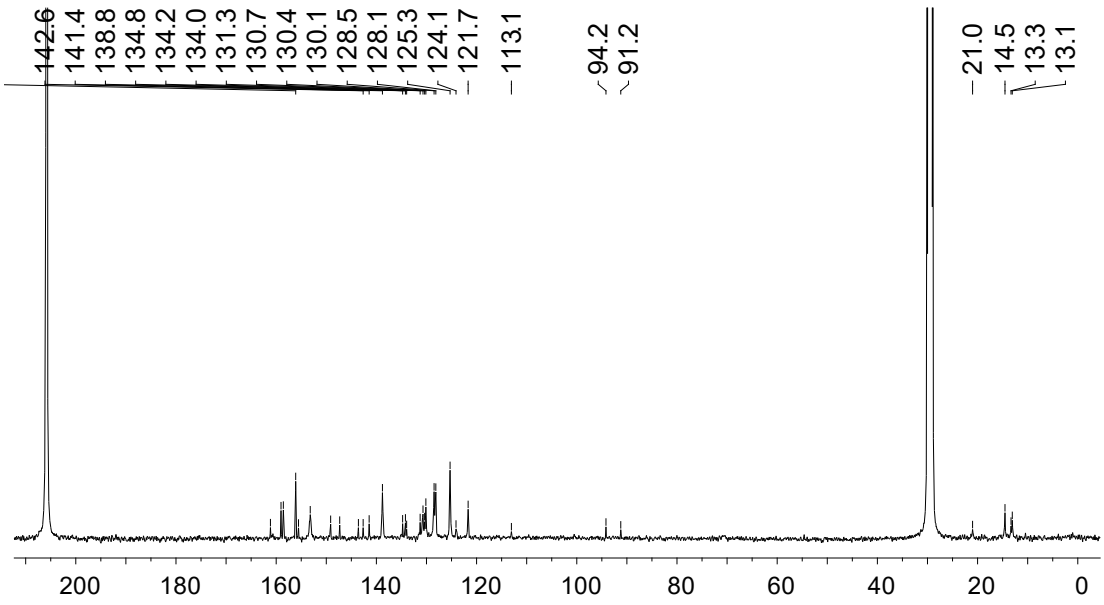

Figure S11. [13]C NMR of **Ru-2** in acetone-d6.

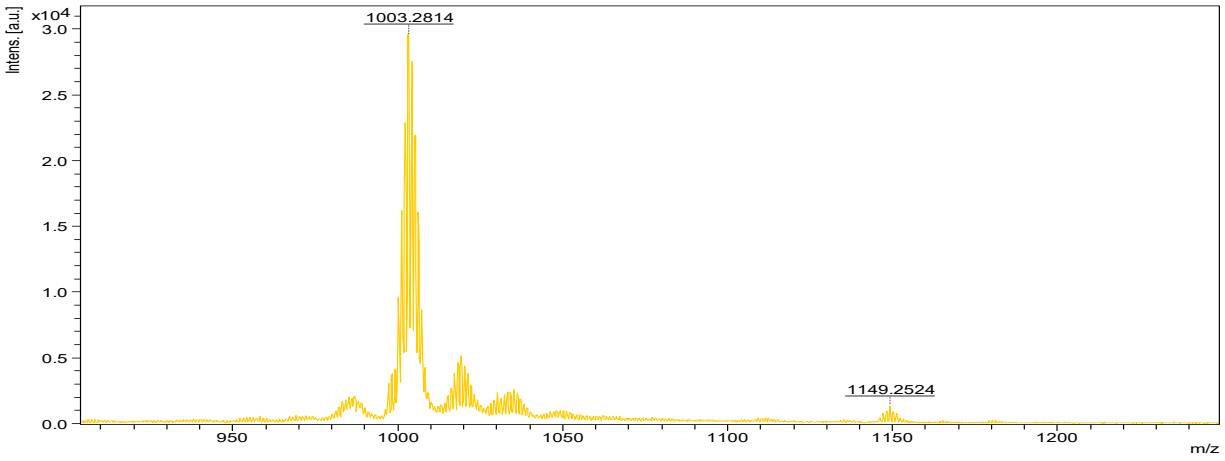

Figure S12. The MALDI-TOF (HRMS) spectrum of **Ru-2**.

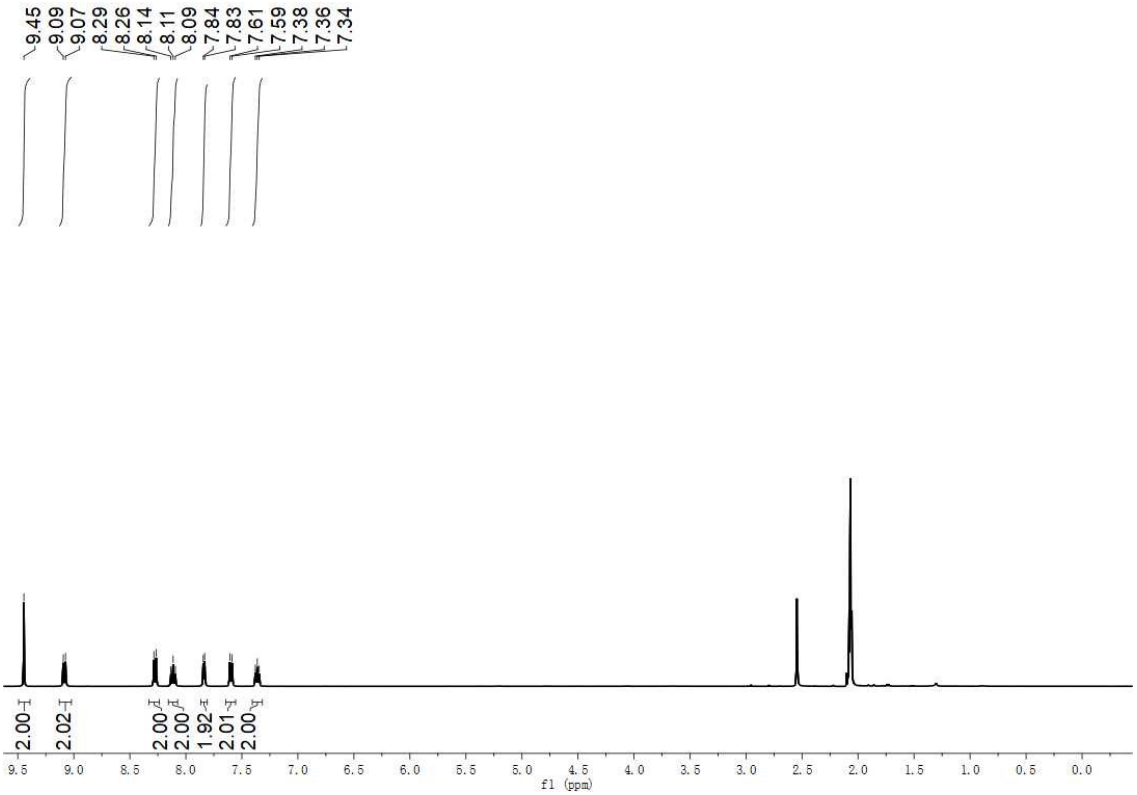

Figure S13**.** [1]H NMR for **Ru-3** in acetone-*d6*, 20℃.

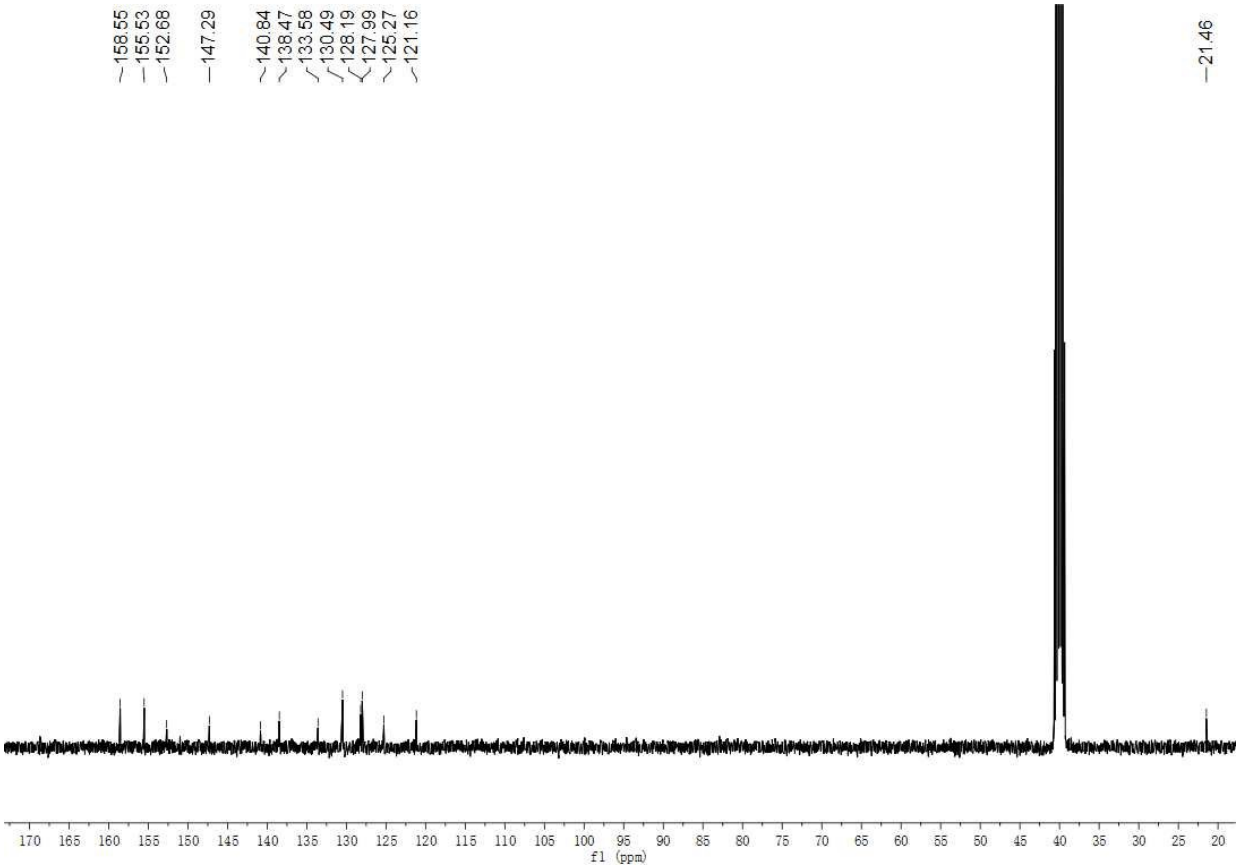

Figure S14**.** ^{13}C NMR for **Ru-3** in DMSO-*d6*, 20℃.

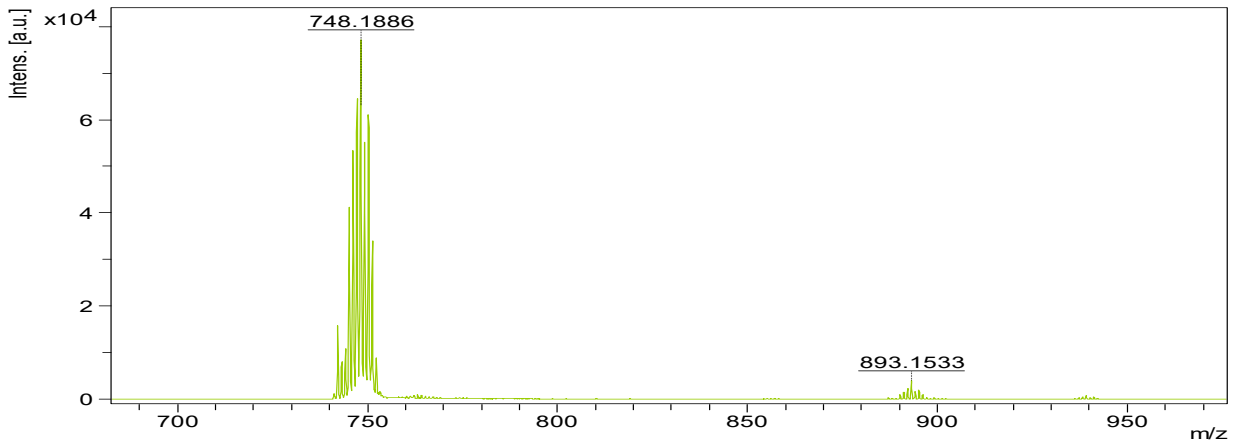

Figure S15. The MALDI-TOF (HRMS) spectrum of **Ru-3**.

3.0 Photophysical details

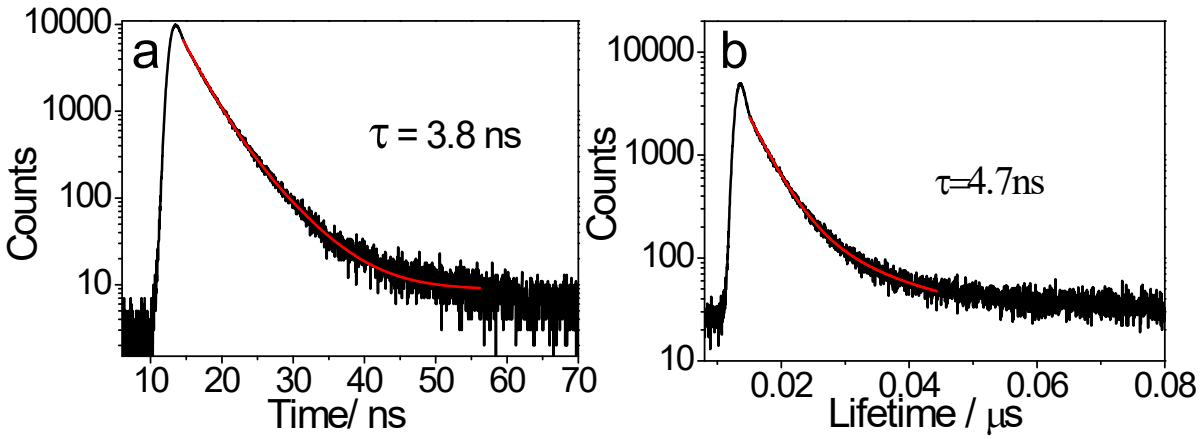

Figure S16. (a) The fluorescence decay spectra **Ru-1** was monitored at 550 nm, 1.0 μM, MeCN, RT; (b) Emission decays of **Ru-2** monitored at 687 nm, 1.0 μM, MeCN, RT.

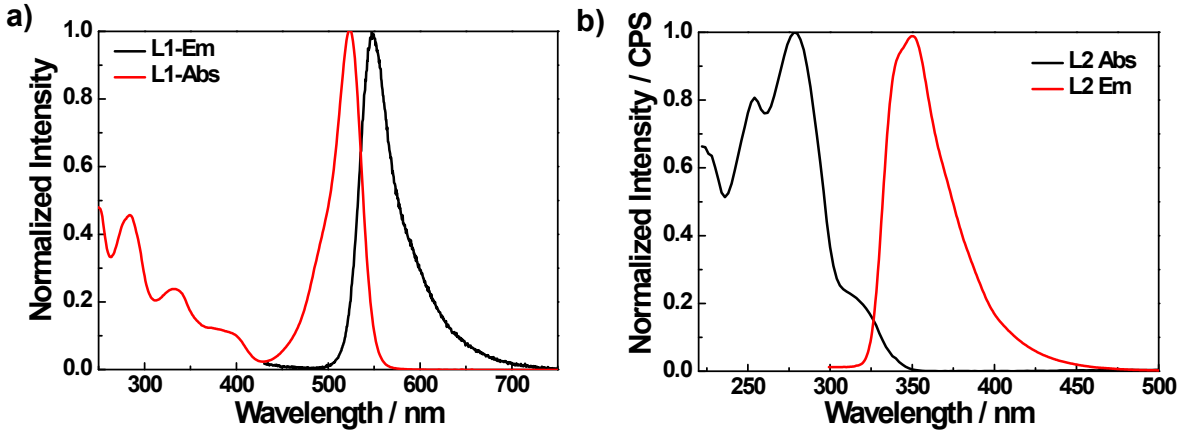

Figure S17. The UV-vis absorption and emission spectra of (a) **L1** and (b) **L2**, 1×10^{-5} M in MeCN, r.t.

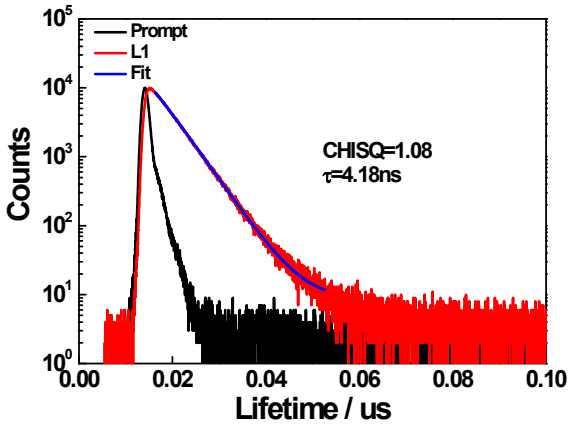

Figure S18. The fluorescence decay spectra **L1** was monitored at 477nm (excited with nanoled 388nm laser) in the MeCN. Experimental conditions: 1×10^{-6} mol/L, RT.

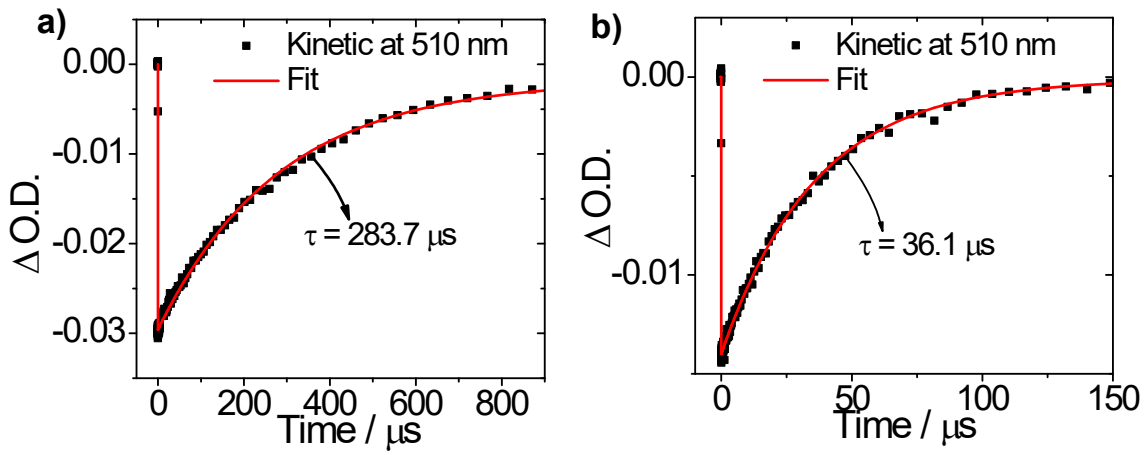

Figure S19. Nanosecond time-resolved transient decay traces of (a) **Ru-1** at 510 nm and (b) **Ru-2** at 510 nm. 2×10^{-5} M in deaerated MeCN, 20℃.

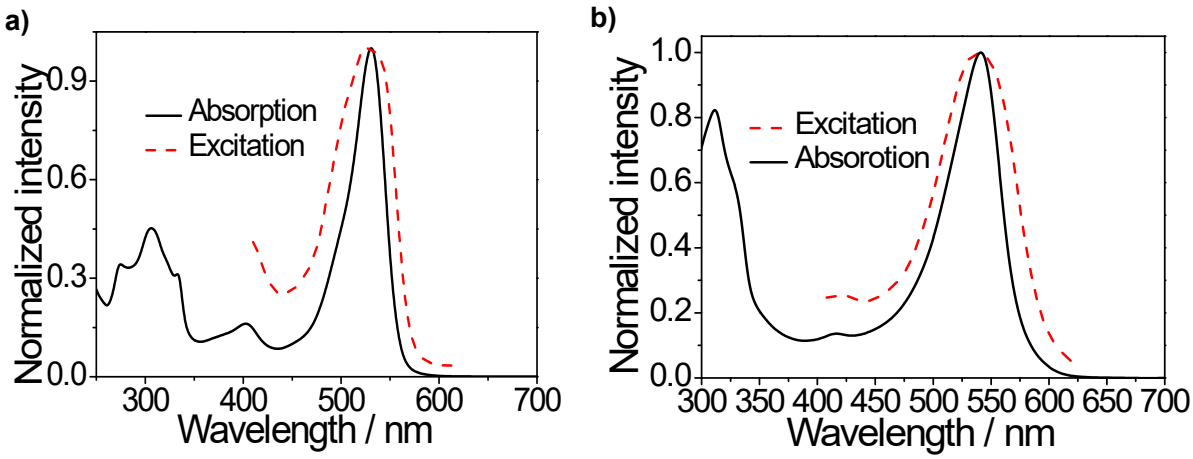

Figure S20. Comparison of the normalized UV-vis absorption and the excitation spectra of the complexes **Ru-1** (a), **Ru-2** (b), λ_{em} = 750nm, 1×10^{-5} mol/L, in MeCN solution, r.t.

4.0 Upconversion details

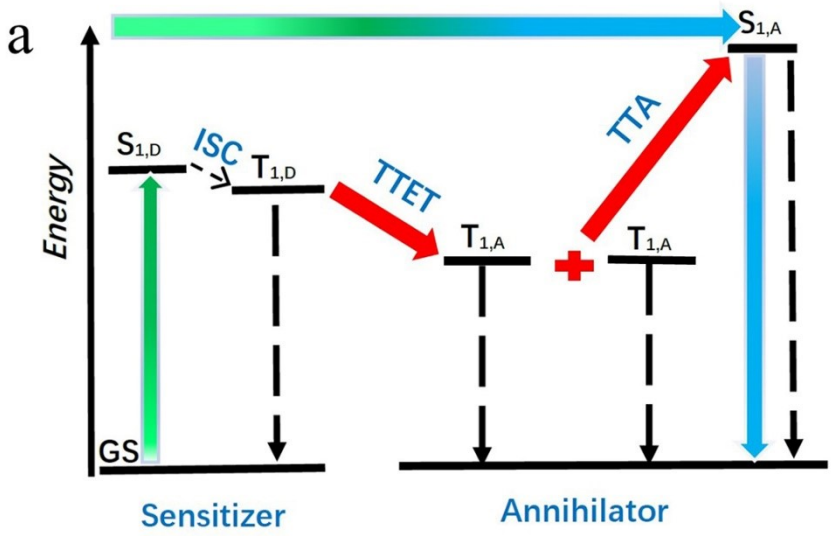

Figure S21. (a) Schematic energy-level illustration of the TTA-UC process. GS, $S_{1,D}$ and $T_{1,D}$ represent the ground state, singlet and triplet excited states of the energy donor (sensitizer), respectively. $S_{1,A}$ and $T_{1,A}$ represent singlet and triplet excited states of the energy acceptor. ISC, TTET, and TTA represent the process of intersystem crossing, triplet−triplet energy transfer, and triplet−triplet annihilation, respectively.

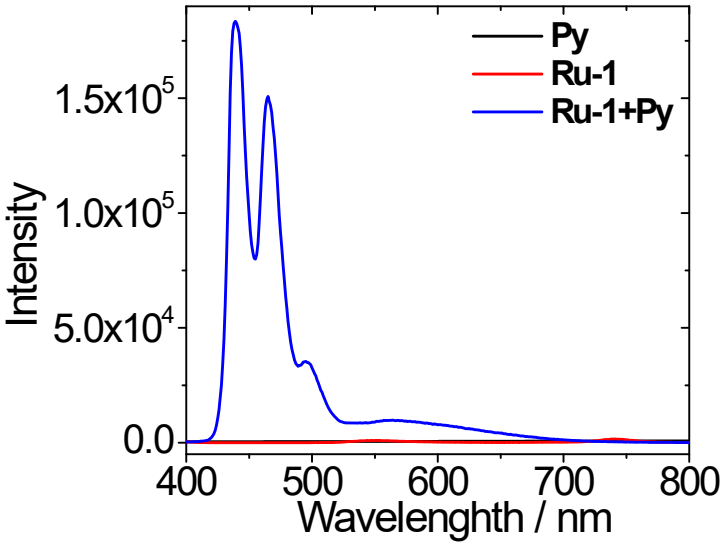

Figure S22. The emission spectra of **Ru-1**, **Py** and the mixture of **Ru-1**/**Py** in the deaerated MeCN, [**Ru-1**] = 1.0 μM, [**Py**] = 3.3 μM, power densitiy = 343.9 mW/cm^2, RT.

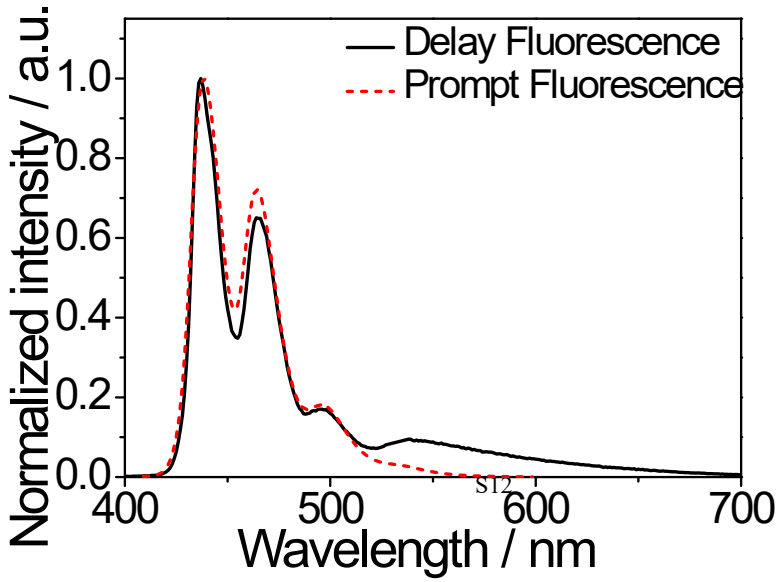

Figure S23. Normalized spectra of UC emission of **Ru-1** / **Py** system and prompt fluorescence of **Py** in MeCN, [**Ru-1**] = 1.0 μM, [**Py**] = 3.3 μM, RT.

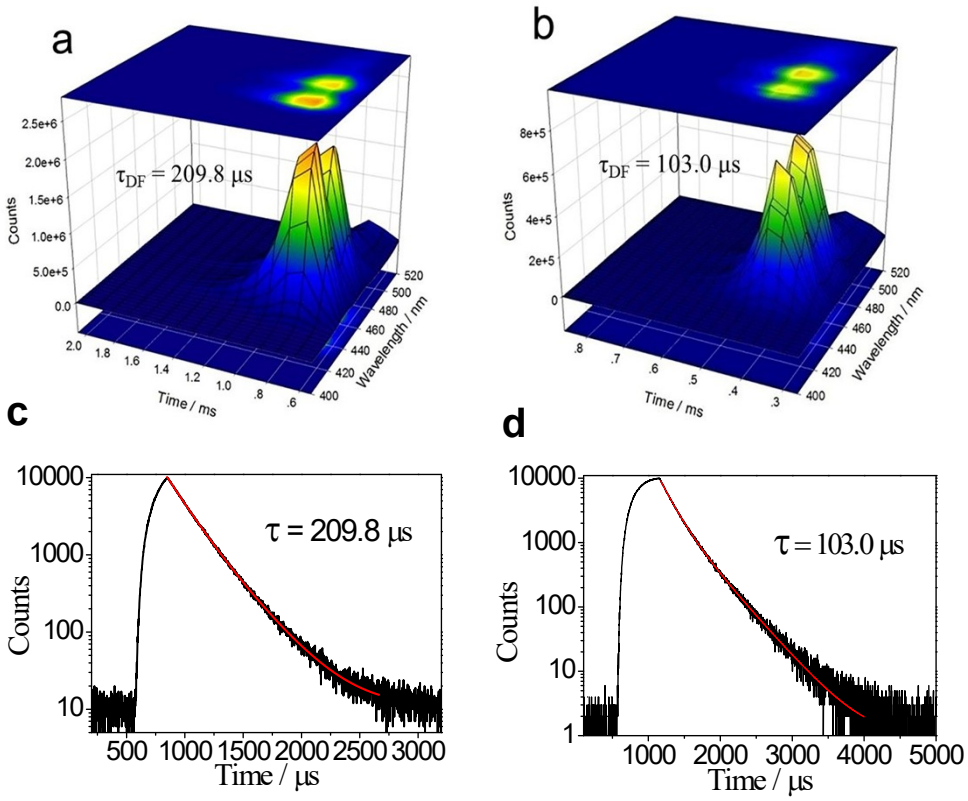

Figure S24. Time-resolved emission spectra (TRES) of the upconverted fluorescence of **Py** using (a) **Ru-1** as the triplet photosensitizer and (b) **Ru-2** as the triplet photosensitizer. Experimental conditions: [**Ru-1**] = 10 μM, [**Ru-2**] = 10 μM, [**Py**] = 33 μM, in deaerated MeCN, RT; The TTA-UC decay spectra of (c) **Ru-1** / **Py** and (d) **Ru-2** / perylene, λ_{em} = 445 nm.

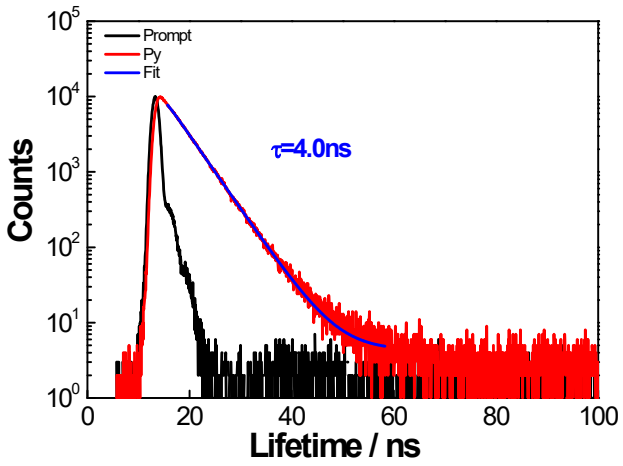

Figure S25. The fluorescence decay spectra **Py** was monitored at 450 nm (excited with nanoled 388nm laser) in the MeCN. Experimental conditions: 1×10^{-5} mol/L, RT.

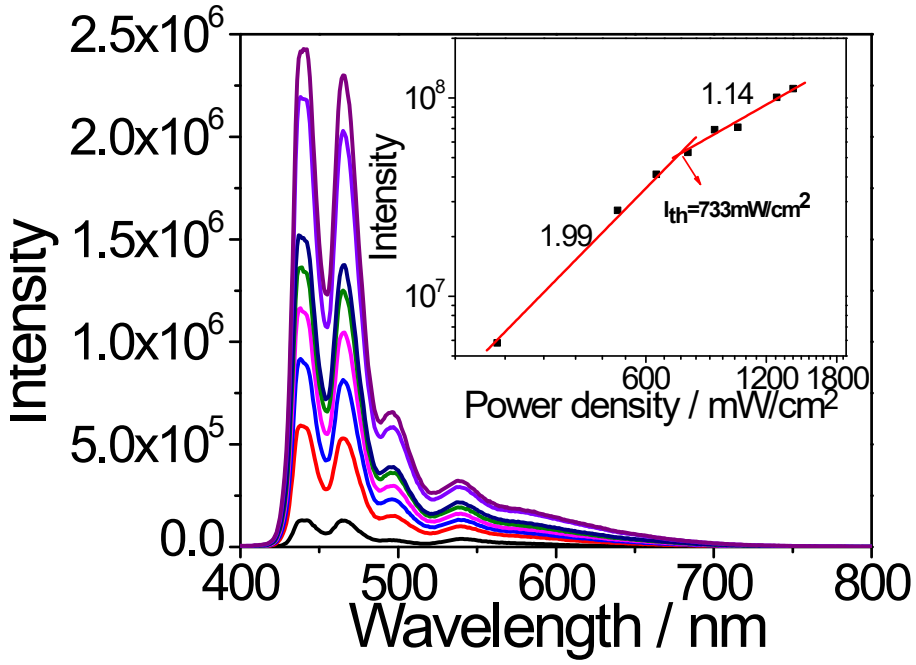

Figure S26. Excitation power dependency of the upconverted perylene emission with **Ru-2** as sensitizers, λ_{ex} = 532 nm, MeCN. (Insert: the normalized integrated emission intensity plotted as a function of normalized incident light power). The minimal and the maximal excitation power densities are 254.8 mW/cm^2 and 1401.3 mW/cm^2, respectively. [**Ru-2**] = 1.0 μM, [**Py**] = 3.3 μM.

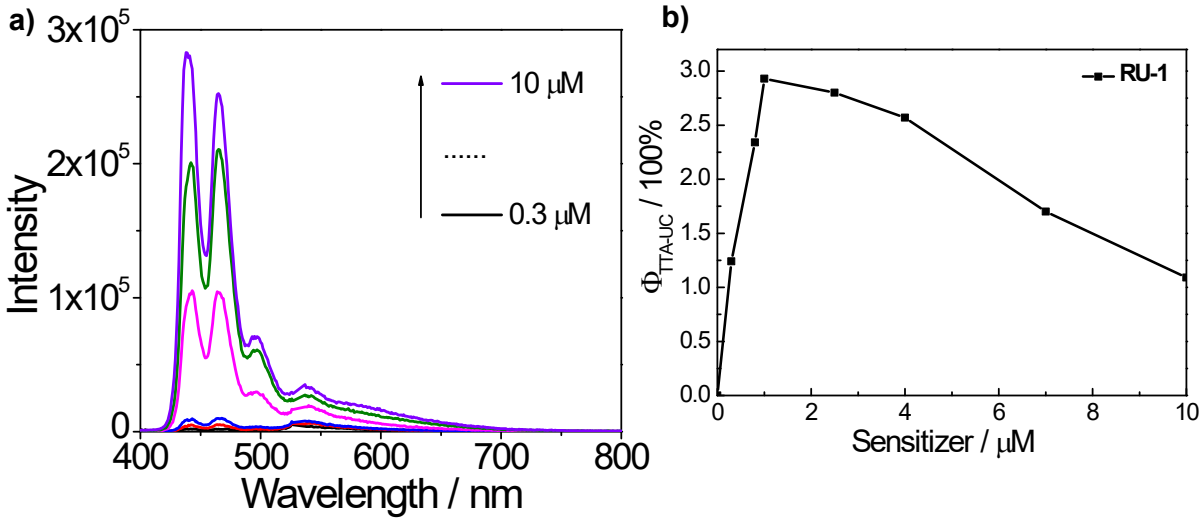

Figure S27. (a) Dependency of the UC emission upon the concentrations of sensitizer **Ru-1** in deaerated MeCN; (b) The upconverted quantum yield plotted as a function of the concentration of **Ru-1**. [**Py**] = 3.3 μM in MeCN. power density = 1273.9 mW·cm^{-2}, λ_{ex} = 532 nm.

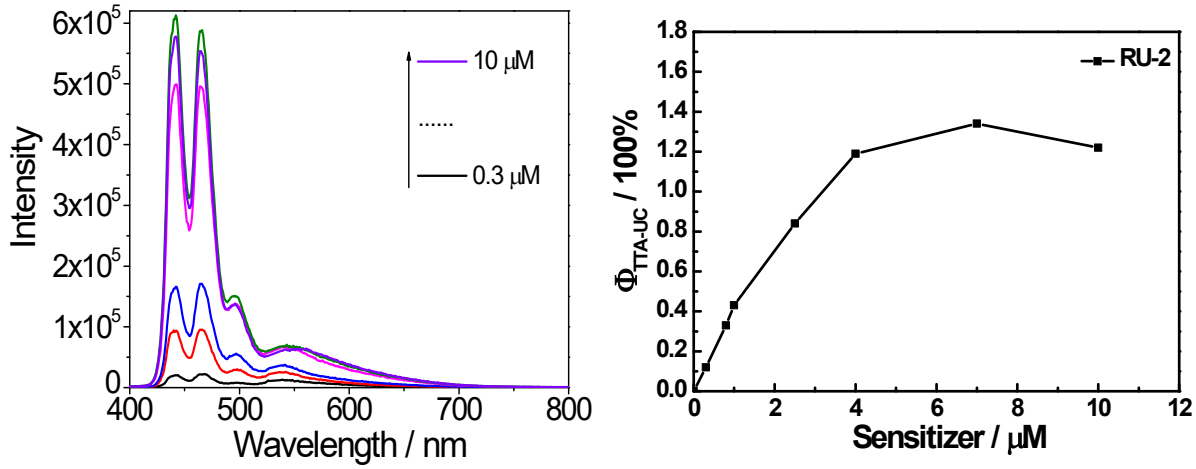

Figure S28. (a) Dependency of the UC emission upon the concentrations of sensitizer **Ru-2** in deaerated MeCN; (b) The upconverted quantum yield plotted as a function of the concentration of **Ru-2**. [**Py**] = 3.3 μM in MeCN. power density = 1273.9 mW·cm^{-2}, λ_{ex} = 532 nm.

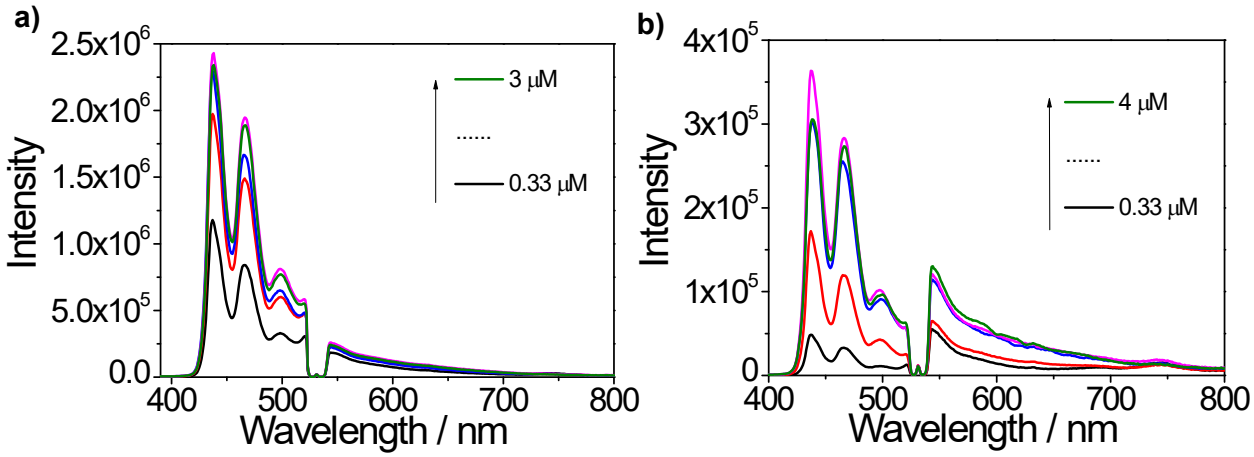

Figure S29. (a) Dependency of UC emission spectra upon the concentrations of acceptor **Py** with (a) **Ru-1** and (b) **Ru-2** as the sensitizers, λ_{ex} =532 nm, [**Ru-1**] = 1.0 μM, [**Ru-2**] = 1.0 μM in deaerated MeCN, power density = 1273.9 mW/cm^2, RT.

Table S1. The quantum efficiency with different concentration of acceptors [a]

	0.33 μM	0.67 μM	1.0 μM	2.0 μM	3.0 μM
$\Phi_{Ru\text{-}1}$	1.29%	2.28%	2.56%	2.93%	2.83%
$\Phi_{Ru\text{-}2}$	0.045%	0.18%	0.38%	0.43%	0.4%

[a] Excited with 532 nm laser, with the prompt fluorescence of **I-BDP-I** as the standard (Φ = 2.7 % in MeCN).

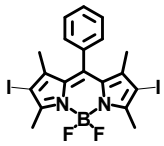

I-BDP-I

Figure S30. The chemical structure of **I-BDP-I**

Table S2. Triplet excited state lifetimes (τ_T), Stern-Volmer quenching constant (K_{SV}) and bimolecular quenching constants (k_q) of **Ru-1**, **Ru-2** and **Ru-3** as the sensitizers. [a]

	K_{sv} (10^3 M^{-1})	k_q (10^9 M^{-1}s^{-1})	τ_{DF} / μs	Φ_{UC} (%)[b]	η [c]/ 10^3 M^{-1}cm^{-1}
Ru-1	3994.2	10.9	209.8	2.93	3.47
Ru-2	683.4	12.7	103.0	0.43	0.22

[a] Excited with 532 nm laser. [b] results with [**sensitizer**] = 1.0 μM, [**Py**] = 3.3 μM. [c] apparent brightness. $\eta = \varepsilon \times \Phi_{UC}$.